AGU PUBLICATIONS

JGR

Journal of Geophysical Research: Earth Surface

RESEARCH ARTICLE

10.1002/2013JF002959

Key Points:
- We model hillslope sediment supply to channels at the reach scale
- Interaction between storms and hillslope attributes affects supplied sediment/GSD
- Hillslope sediment supply impacts channel bed material in dryland basins

Correspondence to:
K. Michaelides,
katerina.michaelides@bristol.ac.uk

Citation:
Michaelides, K., and M. B. Singer (2014), Impact of coarse sediment supply from hillslopes to the channel in runoff-dominated, dryland fluvial systems, *J. Geophys. Res. Earth Surf.*, *119*, 1205–1221, doi:10.1002/2013JF002959.

Received 21 AUG 2013
Accepted 30 APR 2014
Accepted article online 5 MAY 2014
Published online 3 JUN 2014

Impact of coarse sediment supply from hillslopes to the channel in runoff-dominated, dryland fluvial systems

Katerina Michaelides[1] and Michael Bliss Singer[2,3]

[1]School of Geographical Sciences and Cabot Institute, University of Bristol, Bristol, UK, [2]Department of Earth and Environmental Sciences, University of St Andrews, Saint Andrews, UK, [3]Earth Research Institute, University of California, Santa Barbara, California, USA

Abstract Sediment supply from hillslopes to channels is an important control on basin functioning and evolution. However, current theoretical frameworks do not adequately consider processes of runoff-driven hillslope sediment supply, which affect river channels spatially and temporally. Mountainous dryland basins exhibit an important manifestation of these processes because their debris-mantled hillslopes produce coarse sediment and because rainfall is delivered as infrequent, high-intensity, short-duration rainstorms. This paper combines field measurements and modeling to explore runoff-driven coarse sediment supply from hillslopes to the channel and assesses a range of plausible storms on the longitudinal patterns of sediment load and its caliber over a dryland basin reach. Our results show that modeled sediment load and its grain size distribution are determined by the nonlinear interaction between rainfall characteristics and hillslope attributes, resulting in longitudinal fluctuations in sediment supply, the relative magnitude and location of which varies between storms. Results suggest that long hillslopes are most sensitive to rainfall and they exhibit large variations in supplied sediment load and grain size for different runoff characteristics. Short and steep hillslopes are less sensitive to rainfall variations as gradient effects dominate over the role of length in modulating runoff accumulation. Furthermore, the signal of the median fraction (D_{50}) of modeled sediment supplied by the hillslope is preserved in the coarse fraction of the measured in-channel grain sizes (D_{90}). Finally, we propose a simple index, which provides new insights into the effectiveness of different rainstorms in terms of the impact of hillslope sediment supply on the channel.

1. Introduction

Sediment supply to river channels has important consequences for bed-material texture, channel form and functioning, and for downstream depositional records. Generalized understanding of the influence of sediment supply on channels typically emerges from studies in which the upstream supply is isolated; limiting a broader perspective of the role sediment supply plays longitudinally on reach and basin scales. Previous work has investigated upstream supply changes via laboratory experiments [*Dietrich et al.*, 1989; *Gilbert*, 1914; *Iseya and Ikeda*, 1987; *Lisle et al.*, 1993; *Venditti et al.*, 2010], field case studies [*Gilbert*, 1917; *Gomez et al.*, 2001; *Knighton*, 1989; *Singer*, 2008; *Singer*, 2010], and in modeling [*Armitage et al.*, 2011; *Hoey and Ferguson*, 1997; *Paola et al.*, 1992], demonstrating emergent downstream responses. Other work has addressed the impact of individual localized pulses of sediment supply to channels that dissipate through time [*Korup et al.*, 2010; *Lisle et al.*, 1997, 2001] or persist at tributary junctions [*Rice*, 1998, 1999]. However, an important research gap is the characterization of mass and grain size distribution (GSD) of sediment supply to channels within drainage basins that are not simply characterized by one upstream source or that have localized inputs [e.g., *Attal and Lave*, 2006]. Although there are notable examples of research that have explicitly addressed the influence on channels of stochastic hillslope sediment supply by landsliding within an entire drainage basin [e.g., *Benda and Dunne*, 1997b], the local and downstream impacts to channel GSD of hillslope-derived sediment by surface wash processes remain unresolved. Such wash processes on hillslopes occur during rainstorms, and they impose a cumulative impact on channels that is not easily assessed by field observation on event timescales.

In some drainage basins, sediment supply is spatially heterogeneous and variations in the magnitude and caliber of delivered sediment may significantly impact entire river reaches. In lower order river domains and tectonically active basins, hillslopes play an important role in delivering sediment to valley-floor channels [*Attal and Lave*, 2006; *Harvey*, 1991, 2001]. In such systems the communication of sediment from hillslopes to

channels depends on the entrainment of available sediment from slopes, its downslope transit, and the discontinuous buffering of the supplied sediment by varying degrees of topographic coupling between hillslopes and channels [*Harvey*, 2002]. Channel response to hillslope sediment supply at a particular valley cross section depends on the mass and GSD of delivered sediment and on the local transport and sorting of the supplied sediment by channel flow.

Discrete, localized sediment pulses (e.g., landslides) may completely transform a subreach [*Hovius et al*., 2000; *Korup et al*., 2010; *Lisle et al*., 2001; *Madej and Ozaki*, 1996], but the overall longitudinal influence of a single pulse on the channel will typically diminish with distance from the local sediment input according to dispersion theory [*Benda and Dunne*, 1997b; *Lisle et al*., 2001]. Furthermore, the influence of a discrete pulse will wane through time as the river progressively reworks the delivered material. Previous research has emphasized the spatial variability in sediment supply by localized mass wasting [e.g., *Densmore et al*., 1998; *Hovius et al*., 1997, 2000] and by diffuse fine sediment sources from uplands [e.g., *Carson et al*., 1973; *Hicks et al*., 2000]. In contrast, there is currently a lack of physically based, generalized understanding of spatial and temporal variability of coarse sediment delivery from hillslopes by overland flow for drainage basins in which this process is important [e.g., *Rustomji and Prosser*, 2001]. The coarse fraction of hillslope supply is particularly important because it is often incorporated into the channel bed material, providing resistance to flow and bed load flux, and may therefore impact long-term evolution of valley floors.

This paper analyzes the impact of hillslope sediment supply on channel grain size over a river reach. The research is focused on montane, dryland basins where hillslopes are typically sparsely vegetated and covered in thin, noncohesive soils and coarse rock fragments resulting from low rates of chemical weathering [*Carson and Kirkby*, 1972]. Although mean annual rainfall is low, it occurs as infrequent, high-intensity, short-duration rainstorms that are spatially variable and typically smaller in area than the drainage basin (i.e., only parts of the basin are affected) [*Nicholson*, 2011]. These rainstorms, coupled with thin and sparsely vegetated soils, generate patchy and short-lived, yet significant, hillslope runoff [*Yair et al*., 1978], capable of transporting large quantities of sediment to the channel [*Nichols et al*., 2013]. Due to their temporal and spatial variability, these rainstorms produce episodic sediment supply, but the interaction between such storms, overland flow, and hillslope attributes in coarse-mantled dryland basins is not well understood, in contrast to other environments [*Benda and Dunne*, 1997b; *Gabet and Dunne*, 2003].

The challenge presented is to quantify sources of coarse hillslope sediment to channels that are small for individual events but which have important cumulative impacts to dryland fluvial systems [*Nichols et al*., 2013]. This research has implications for adapting landscape evolution models for operation on transient timescales, for increasing understanding of longitudinal grain size trends in channels that interact with hillslopes, and for generating hypotheses about relative erosion rates between slopes within a particular basin. Here we combine a field- and modeling-based approach in order to quantify rainstorm-driven sediment supply to valley floors and to assess the impact of this supply on longitudinal grain size characteristics within a coarse-mantled, dryland basin in southeastern Spain. Specifically, we explore the interaction between climatic forcing and the spatially variable basin characteristics that affect sediment supply patterns and we test the hypothesis that over a series of plausible storms the hillslope sediment signal can be detected in the channel grain size distribution at the reach scale.

2. Field Site

Data were collected from the Nogalte catchment (Figure 1), a 171 km^2 basin located on the border of the Provinces of Murcia and Almería of Spain. This basin is underlain by mica schist and bounded by convex hillslopes subject to creep, wash, and rill erosion. It is drained by the 33 km Rambla de Nogalte, an ephemeral, sand, and gravel-bedded river. The climate of the region is semiarid with low annual rainfall (mean = 300–400 mm yr^{-1}) that occurs during infrequent convective rainstorms, in which large floods recur somewhere between 7 and 11 years [*Bull et al*., 1999; *Thornes*, 1977] based on limited data typical of dryland areas [*Nicholson*, 2011]. Rainstorms with rainfall intensities up to 200 mm h^{-1} with durations of ~15 min are not uncommon in this catchment [*Bull et al*., 1999]. The channel meanders within the valley floor and floodplains tend to disconnect hillslopes from the channel on alternate sides of the valley (Figure 2a), yielding hillslope-channel disconnection on at least one side of the valley for most sections (Figure 2c), as well as totally disconnected (Figure 2d) and fully connected (Figure 2b) parts of the reach. Soils on the hillslopes are thin

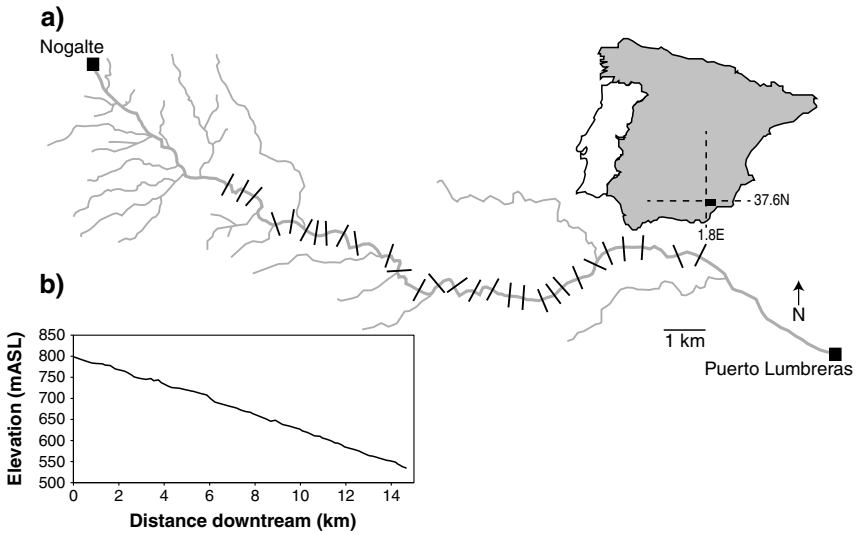

Figure 1. (a) Map of the study site showing the Rambla de Nogalte and the location of the cross sections. (b) Channel long profile with a reach-averaged gradient of 0.019 and a standard error of 0.001 m.

and stony, and vegetation cover is sparse. Land use within the basin is a mixture of cultivated orchards (almonds and olives) and Mediterranean shrubs.

3. Field Methods and Data

Topographic valley cross sections and hillslope and channel particle sizes were measured at 29 longitudinal locations along a 15 km reach of the middle Nogalte approximately every 500 m (Figure 1). At each transect, coarse hillslope surface particle sizes (>2 mm) were measured at 10 m intervals downslope from the crest to the floodplain or channel interface yielding ~1000 hillslope data points in total over the study reach. For each hillslope particle sampled, dry weight and all three axes (D_a, D_b, and D_c) were measured in order to determine mass and shape characteristics.

Channel grain sizes were recorded at 0.5 m intervals across the channel (averaging 100–400 points per cross section depending on the width), measured by surface pebble counts (intermediate axis) for half phi grain

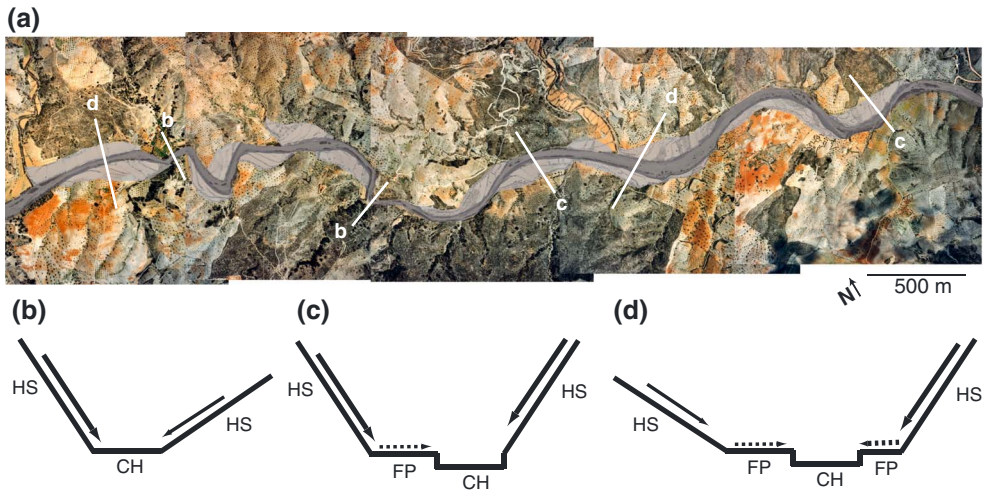

Figure 2. (a) Aerial photograph of a section of the Nogalte showing the main channel (dark grey), adjacent floodplains (light grey), and hillslopes. The white lines denote example sections depicted in the schematics below. (b) A topographically coupled section; (c) a partially topographically coupled section; and (d) a topographically decoupled section. HS is hillslope, FP is floodplain, and CH is channel.

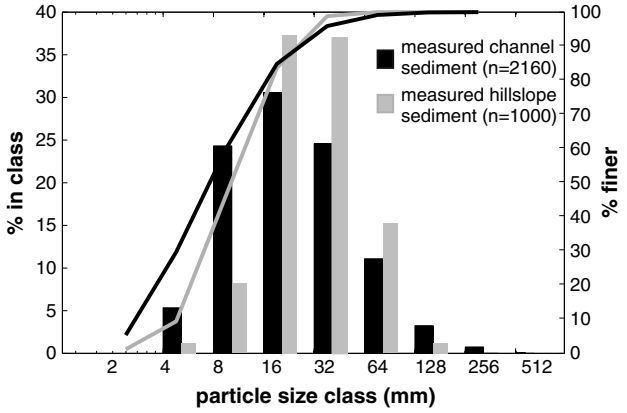

Figure 3. Frequency (bars) and cumulative (curves) grain size distributions of measured hillslope and channel sediment based on the intermediate axes (D_b), where n denotes the number of particles used to derive each distribution.

size classes between 2 mm and 512 mm using the Wolman method [*Wolman*, 1954]. Lateral limits of the channel were defined as significant breaks in cross-valley slope. GSDs were analyzed using GRADISTAT software [*Blott and Pye*, 2001] by logarithmic method of moments to obtain characteristic grain sizes (D_{10}, D_{50}, and D_{90}) and sorting coefficients. Figure 3 shows GSDs of the measured channel and hillslope sediment. It highlights that the hillslope surface is coarser than the channel, with a D_{50} of 36 mm compared to 25 mm, respectively. The Zingg plot (Figure 4) of hillslope particles, based on measured data of all three axes, illustrates that there is no single dominant particle shape on the hillslopes. Particles fall into all four shape categories, with a higher number of blade- and rod-type shapes, which might be expected for a schist basin.

The channel long profile is straight (Figure 1b), and the reach-averaged (over 15 km) local bed slope is 0.019 (standard error = 0.001 m). Hillslope lengths, floodplain, and channel width all fluctuate over the reach, but there is an overall valley width increase with distance downstream (Figure 5).

Infiltration rates on the hillslopes and floodplains were measured using a single-ring infiltrometer. A total of 30 infiltration tests were carried out on eight hillslopes and two floodplains. These tests were conducted on surfaces under differing land uses, including cultivated (almond and olive) slopes and floodplains, as well as uncultivated (shrub-dominated) surfaces, and each test was triplicated. Each set of measured infiltration data was fitted to the modified *Green and Ampt* [1911] model, which describes the decline in infiltration rate as a result of filling a fixed soil moisture store:

$$f = A + \frac{B}{t} \tag{1}$$

where f is the infiltration rate (mm h^{-1}), A is the final infiltration rate under saturated conditions (mm h^{-1}), B is the initial infiltration under unsaturated conditions (mm), and t is time (h). This equation has been shown to be a good descriptor of infiltration on semiarid slopes [*Scoging*, 1992; *Thornes and Gilman*, 1983]. The derived A and B infiltration parameters vary widely between different land uses. The A values in each land use type, averaged from the triplicate tests, ranged from 15 to 150 mm h^{-1}, and B ranged from 20 to 500 mm.

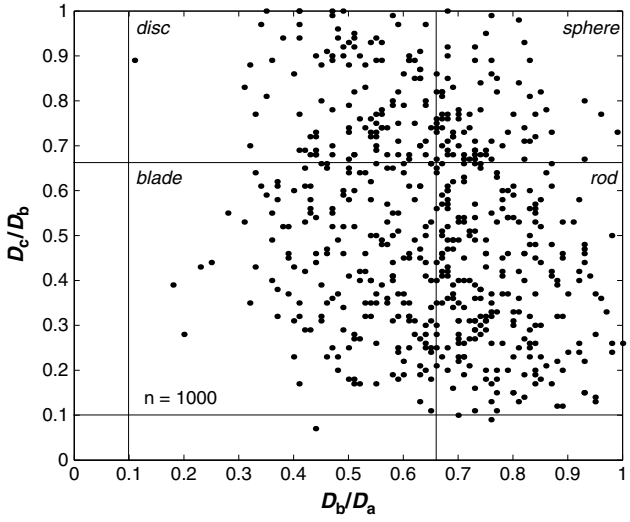

Figure 4. Zingg plot of hillslope particles, where D_a, D_b, and D_c refer to the large-, intermediate-, and small-particle axes, respectively.

4. Modeling Hillslope Sediment Supply to the Channel

We employed a sediment transport model, COUP2D, developed in *Michaelides and Martin* [2012] to simulate the supply of coarse sediment

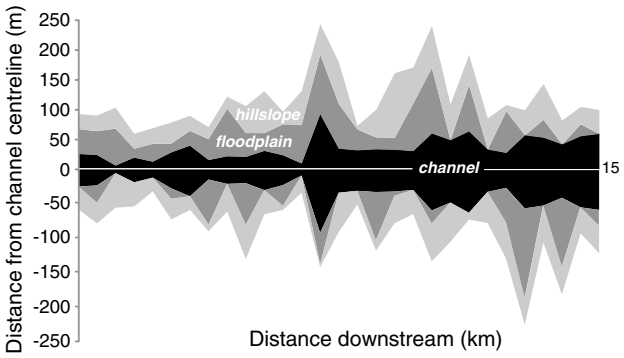

Figure 5. Longitudinal variations in channel width, floodplain width, and hillslope length within the study reach plotted as a distance from an arbitrary channel centerline derived as the channel width/2.

from hillslopes to the channel during rainfall events. The model is runoff driven and employs a particle-based approach for sheetwash sediment transport on debris-mantled hillslopes. The sediment transport component is based on force-balance principles applied to discrete, coarse particles (>1 mm) in multiple size classes. The model explicitly represents surface GSD on the hillslope and calculates particle fluxes and transport distances. It is driven by dynamic drag and lift forces that are induced by fully or partially submerged flow conditions derived from the computed runoff flow hydraulics. The total number of particles is defined as an initial condition within each model run, and no new particles are added to the hillslope profile, based on the assumption that during a single rainfall event no new surface material is being prepared by weathering or other processes.

Runoff generation is derived from the modified *Green and Ampt* [1911] infiltration equation (equation (1)) and represents infiltration-excess and saturation-excess overland flow as a result of filling a fixed soil moisture store [*Michaelides and Wainwright*, 2002; *Michaelides and Wilson*, 2007; *Michaelides and Wainwright*, 2008]. Runoff is routed on a high-resolution (0.1×0.1 m^2) 2-D rectangular grid (hillslope length $\times$ 2 m width) using the kinematic wave approximation, rated using the Manning's n friction factor, with cell to cell flow routing defined by a steepest descent algorithm. COUP2D produces spatial values of runoff flow depths and velocities which constitute the driving force for the particle transport model.

The underlying premise of the sediment transport model is that coarse particles on steep slopes are subjected to forces exerted by runoff and gravity resulting in their gradual movement downslope depending on the grain size and overland flow characteristics (depth, velocity, and duration). Coarse particles have a range of stabilities on the hillslope depending on their size relative to that of the average hillslope surface, so runoff will have varying degrees of effectiveness in transporting grains of different sizes. In the model, the angle of repose of each particle is calculated using the formulation developed in *Miller and Byrne* [1966]:

$$\phi_o = a\left[\frac{D}{k_b}\right]^{-\beta} \tag{2}$$

where ϕ_o is the particle angle of repose, D is effective particle diameter (m), a is a coefficient which depends on particle shape, k_b is the mean diameter of the underlying bed grains (m), and β expresses particle sorting. The coefficient (a) and the exponent (β) account for particle shape and sorting and allow for the characterization of different bed conditions. In these model simulations, we use a value of $a = 55.2$ and $\beta = 0.31$ obtained in *Kirchner et al.* [1990], which represent poorly sorted, rounded to angular sediments and which yield relatively high particle angles of repose (ranging between ~20 and 60° depending on grain size). Shape has been found to exert an important control on particle friction angle [*Li and Komar*, 1986; *Miller and Byrne*, 1966], so assuming sphericity for this schist-dominated field area would likely overestimate sediment supply and GSD of delivered material, especially considering that particles tend to deviate significantly from spheres (see Figure 4).

Depending on the flow depth relative to the particle diameter, the model accounts for lift and drag forces (fully submerged flows) or for the drag force only (partially submerged conditions when flow depth is less than particle diameter). On each particle and at each time step, the relative particle submergence is evaluated and the respective forces (lift, drag, and gravity) are calculated based on the computed runoff hydraulics. In the model the forces acting on each particle are resolved and used to determine if it moves based on

$$F_r = \frac{F_d + F_l + F_g(\sin\theta)}{(F_g\cos\theta)\tan\varphi_o} \tag{3}$$

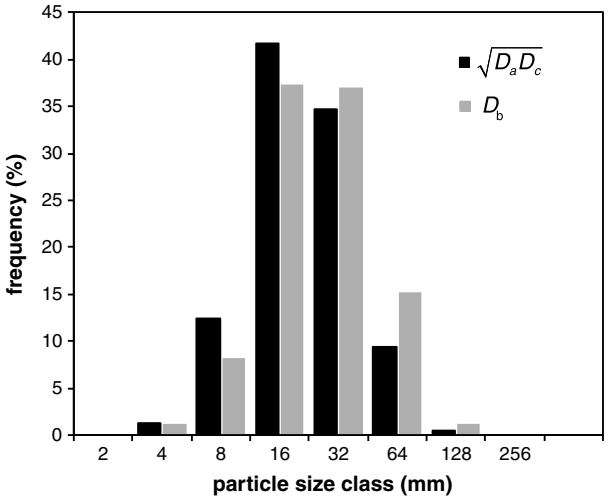

Figure 6. Comparison of hillslope GSDs derived from the particle b axis (D_b) and an effective particle diameter derived from the *a* and *c* axes based on $\sqrt{D_a D_c}$ from *Komar and Li* [1986]. The distribution of D_b axis is coarser than the distribution of $\sqrt{D_a D_c}$ with a D_{50} of 34.07 mm and 29.27 mm, respectively.

where F_r is the resultant force (dimensionless), F_d is the drag force (N), F_l is the lift force (N), F_g is the gravitational force (*N*), tan ϕ_o is the coefficient of static surface friction acting on a particle resisting movement, and θ is the hillslope gradient (°). If $F_r \geq 1$, then transport occurs, and travel distance (*dx*, m) for a particle of mass *m* is calculated in its time derivative form as:

$$d^2x = \frac{F}{m}\, dt^2 \qquad (4)$$

where *F* (*N*) is the detaching force acting on the particle (numerator of equation (3)) and *dt* is the model time step (s). Full details of the model can be found in *Michaelides and Martin* [2012].

In this paper, in order to represent particle shape in the model without explicitly incorporating all three axes for each particle, we used an empirical relationship between mass and frontal area produced from our field data. This area-mass relationship is employed in the model within a particle generation routine in conjunction with a user-defined distribution of characteristic grain diameters to derive individual particle sizes and masses. The empirical relationship converts field-measured grain diameters to particle frontal areas and the corresponding masses. Frontal area is important for force-balance models because it defines the area over which drag and lift forces act on the particle and an overestimation of it could result in higher sediment transport rates. It has been shown that for irregularly shaped, nonspherical particles, a better approximation of projected frontal area is obtained by using D_a (long) and D_c (short) instead of using D_b (intermediate axis) [*Komar and Li*, 1986]. Therefore, we used a distribution of $\sqrt{D_a D_c}$ to represent "effective" particle diameter, and frontal area is calculated as $\pi\left(\frac{D_a D_c}{4}\right)$ [*Komar and Li*, 1986]. Figure 6 shows the two distributions and illustrates how D_b and $\sqrt{D_a D_c}$ compare.

A power law relationship exists between particle frontal area and particle mass with an equation $y = 2.99x^{1.31}$ ($R^2 = 0.90$). The range of values from this fit within the 95% confidence limits for the coefficient (2.621–3.368) and exponent (1.268–1.357) was used to stochastically generate a mass value in the model for a given frontal area. This ensures that particles of a given characteristic diameter do not have exactly the same masses and therefore introduces some variability to compensate for shape variations.

The model was employed on valley topographic cross sections that represent either a hillslope-channel or hillslope-floodplain-channel configuration. We used a down-valley gradient of zero; therefore, transport of particles was simulated down the hillslope to the channel in one dimension along the entire cross section (including the floodplain). Hillslope and floodplain attributes (length/width and gradient) were taken from field measurements and are shown in Table 1.

4.1. Model Simulations

The model was applied to each of the 29 measured cross sections incorporating hillslopes and floodplains (if present) on both sides of the valley (see Table 1), driven by a range of rainfall intensities/durations and infiltration rates based on published and measured data for the Nogalte catchment (Table 2). This resulted in a total of 638 model simulations. Rainfall totals were kept constant, and the same initial hillslope GSD was used in all simulations based on the global (all measured particles) GSD from all hillslopes in the catchment (Figure 6). Infiltration rates were varied for all hillslopes/floodplains uniformly in order to isolate the sensitivity to this parameter. The initial number of particles seeded on the hillslopes (3000 particles/m^2) was scaled by the length of each hillslope, such that the total number of particles per unit length of hillslope was equal. Generated particles were scattered randomly on the hillslope grid at the start of each simulation, ensuring that there are no

Table 1. Measured Valley Cross-Section Data Used in the Model[a]

Distance Downstream (m)	Channel Width (m)	N. Hillslope Length (m)	N. Hillslope Gradient (°)	N. Floodplain Width (m)	N. Floodplain Gradient (°)	S. Hillslope Length (m)	S. Hillslope Gradient (°)	S. Floodplain Width (m)	S. Floodplain Gradient (°)
0	53	33	17	0	n/a	25	19	42	0.5
816	50	30	23	25	0.4	26	11	40	1.5
980	14.5	50	20	0	n/a	35	19.3	62	0
2,220	41	35	25	0	n/a	25	20	15	0.7
2,580	27.5	20	16	0	n/a	26	12	30	1
2,803	58.5	30	13	0	n/a	35	21	25	0.3
3,198	81	20	16.6	65	0.6	25	22	35	1.2
3,738	33	10	30	0	n/a	20	15	80	1
4,513	45.5	40	10	60	0	20	12	40	3
4,947	43.5	50	33	0	n/a	45	21	30	0.5
5,307	63.5	35	13	30	1.3	70	15	52	0.8
6,287	49	6	32	0	n/a	21	18	65	0
6,695	21.5	25	22	45	1.3	56	11.3	100	1.2
7,401	186.5	5	25	0	n/a	51	20	75	5
7,936	71	57	32	0	n/a	70	20	35	1.1
8,944	65.5	20	20	70	0.5	6	16	20	1.5
9,579	69	15	23	6	6	46	20	20	2
10,126	67.5	40	75	0	n/a	108	13	80	0.9
10,673	63	35	17	19	1.3	60	19	110	1.5
10,913	122	55	12	0	n/a	70	26.8	0	n/a
11,216	99.5	57	23	0	n/a	60	28	78	0.6
11,585	129	10	41	0	n/a	50	22	0	n/a
11,865	68.5	45	22	50	2	52	28	70	1.7
12,457	57	53	20	130	1.2	10	85	0	n/a
12,905	116	39	18	0	n/a	42	13	30	1.2
13,231	108	54	26.5	100	2.5	60	30	0	n/a
13,845	85.5	40	25	0	n/a	40	25	20	0
14,235	113	38	16	23	0.2	29	10	0	n/a
14,705	120.5	40	25	0	n/a	40	25	30	0

[a]If there is no floodplain present, then Floodplain Width has a value of zero and Floodplain Gradient is denoted by n/a (not applicable).

biases in transport based on initial grid positions. For each simulation we obtained the total sediment load (kg) supplied to the channel from the hillslope or hillslope-floodplain section (total sediment fluxed over each rainfall event), and the GSD of this sediment was calculated based on number of supplied particles in each size class. At each valley cross section, the total sediment loads and GSDs of supplied sediment from both hillslopes were combined into individual values of load and GSD. We did not have accurate measurements of coarse particle cover for all the hillslopes modeled. Therefore, modeled sediment load depends on the number of particles initially seeded on the hillslope, so it is not an absolute value that can be compared with measured flux. However, assuming all hillslopes have a similar cover fraction of coarse fragments, our modeled sediment loads can be used in a relative sense to identify differences in supply "potential" from each hillslope.

Since we lack data on rates and GSD of sediment supply to the Nogalte upstream of our study reach, we made no assumptions about the source (and transport history) of bed material at each cross section modeled. Instead, we simulated longitudinal hillslope coarse sediment supply to the channel for each set of hydrological conditions and compared the envelope of modeled hillslope-derived GSDs to the measured longitudinal channel GSD. The model is not calibrated in any way to produce results that fit the observed channel data; it simply uses a realistic range of physical parameters for the catchment to gain insight into coarse hillslope sediment supply to channels by overland flow.

5. Results

5.1. Total Sediment Load From Hillslopes to Channel

Total sediment load supplied from hillslopes to the channel varies significantly within the reach and between rainfall events (Figure 7). The longitudinal variation in sediment load for various rainfall events arises due to differences in hillslope gradients and lengths and to the presence or absence of floodplains. The presence of a floodplain, regardless of its gradient or width, prevents the transport of all coarse particles from the hillslope to

Table 2. Variables and Constants Used in the Model Simulations

Variables and Constants		
	Hydrological Variables	
Rainfall Intensity (mm h^{-1})	Rainfall Duration (mins)	Final Infiltration Rate, *A* (mm h^{-1})
25[a]	60	15
50[a]	30	15
100[a]	15	15
		50
200[a]	7.5	15
		50
		150
400[b]	3.75	15
		50
		150
	Model Variables That Remained Constant/Constants	
Initial infiltration, *B* (mm)		162
Hillslope width (m)		2
Grid cell size, *dx* (m)		0.1
Time step, *dt* (s)		0.1
Lift coefficient ratio		0.8
Manning's friction *n*		0.04 (hillslope)
		0.06 (floodplain)
α		55.2
β		0.31
k_b (mm)		4

[a]Denotes values obtained from *Bull et al.* [1999] and *Bracken et al.* [2008] for the Nogalte.
[b]Denotes a chosen extreme storm (of very low duration) that has not been recorded but could occur in this area. Final infiltration rates are based on the range of measured field data (15–150 mm h^{-1}).

the channel, so cross sections with floodplains on both sides of the channel produce zero sediment supply. Even the floodplain with the steepest lateral slope (2.5°) does not yield any particles to the channel. In sections with no floodplain, hillslope gradient and length strongly affect runoff characteristics and therefore impact sediment supply. The combination of floodplain sediment buffering and spatial variation in hillslope attributes results in discontinuous and fluctuating hillslope sediment supply along the channel reach, regardless of the rainfall characteristics.

Figure 7 shows that variation in hydrological conditions (i.e., different combinations of rainfall intensity/duration and infiltration rate) can shift the relative magnitude of peaks in sediment supply up and down the reach. At relatively high runoff rates (generated by low infiltration) the highest peak in sediment load occurs

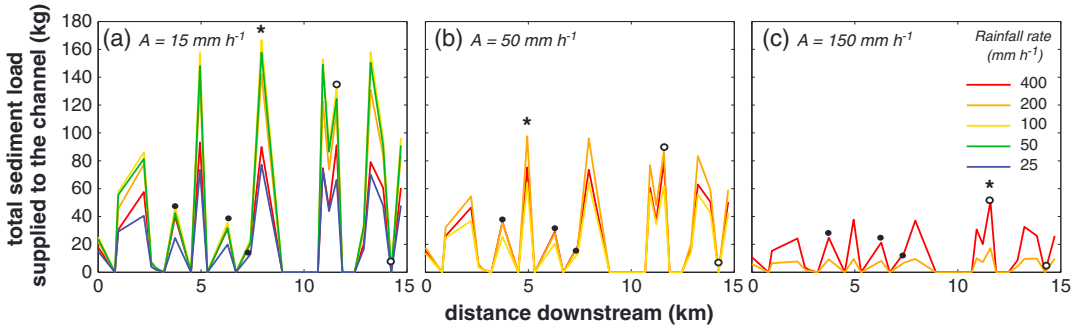

Figure 7. Longitudinal variations in modeled total sediment load per unit hillslope width for different rainfall intensities and durations for (a) $A = 15$ mm h^{-1}, (b) 50 mm h^{-1}, and (c) 150 mm h^{-1}, where *A* is final infiltration rate. The duration for each rainfall intensity are 400 mm h^{-1} (3.75 min), 200 mm h^{-1} (7.5 min), 100 mm h^{-1} (15 min), 50 mm h^{-1} (30 min), and 25 mm h^{-1} (60 min). The asterisk denotes the locations where hillslopes supplied the highest mass of sediment in the reach. Closed and open circles refer to grain size enrichment ratio (ER) responses presented in Figure 8 (for reference).

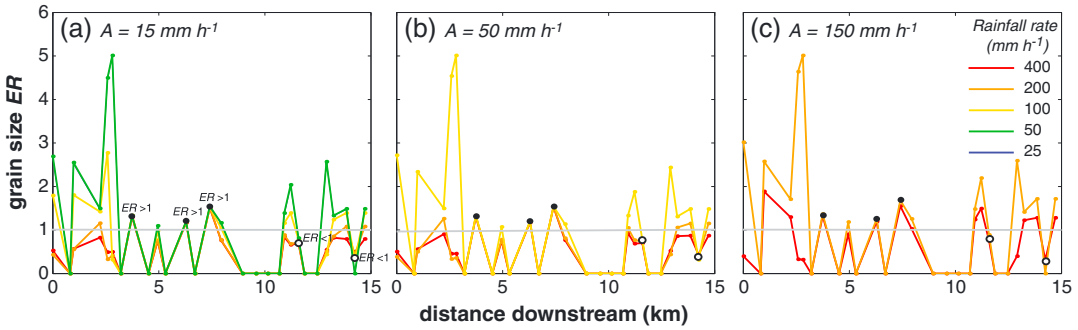

Figure 8. Longitudinal variations in modeled grain size enrichment ratio (ER) for different rainfall intensities and durations for (a) $A = 15\ \mathrm{mm\ h^{-1}}$, (b) $50\ \mathrm{mm\ h^{-1}}$, and (c) $150\ \mathrm{mm\ h^{-1}}$, where A is final infiltration rate. ER is defined as the D/D_{50}, where D is the supplied grain size and D_{50} is the median grain size of the initial hillslope distribution. The grey line denotes ER = 1 (supplied D_{50} = initial hillslope D_{50}). Closed circles denote the locations where hillslope ER is always > 1, and open circles denote the locations where ER is always < 1, under the scenarios modeled.

at 8 km (Figure 7a), whereas at moderate runoff rates it occurs at 5 km (Figure 7b) and at 11 km for low runoff rates (Figure 7c). The highest supplied sediment loads are not necessarily attained by the highest intensity or the longest duration rainfall event. Figure 7a highlights that sediment loads are highest at $100\ \mathrm{mm\ h^{-1}}$ (for 15 min) rainfall and lowest at $25\ \mathrm{mm\ h^{-1}}$ (for 1 h). At low infiltration rates (e.g., $15\ \mathrm{mm\ h^{-1}}$), all of the rainfall intensities simulated produce high runoff rates on the hillslopes, which results in the effective transport of sediment. In these cases, however, since runoff is relatively high for all rainfalls, duration becomes important as it controls how far and for how long sediment can move downslope. In Figure 7a, therefore, the highest rainfall intensity ($400\ \mathrm{mm\ h^{-1}}$) does not produce the highest sediment loads because of the correspondingly short storm duration (3.75 min), which precludes the accumulation of runoff downslope and reduces transport time. This effect is especially important for longer hillslopes. In contrast, the $100\ \mathrm{mm\ h^{-1}}$ rainfall produces the highest peak in sediment load because it is the storm which, for that particular infiltration rate, produces the most effective runoff rates for the longest amount of time. In other words, the $100\ \mathrm{mm\ h^{-1}}$, 15 min duration storm hits a "sweet spot" for sediment transport (for that infiltration rate) across most of the hillslopes in the basin. However, the effectiveness of rainstorms changes with increasing infiltration rate. Under high infiltration rates ($150\ \mathrm{mm\ h^{-1}}$) most rainstorms do not produce runoff and for the storms that do, runoff depth, not duration, becomes the limiting factor. Hence, as is shown in Figure 7c, the $400\ \mathrm{mm\ h^{-1}}$ storm produces the highest sediment loads with the largest peak occurring at 11 km (as opposed to 8 km and 5 km for the other two infiltration scenarios).

These complex dynamics occur as a result of the nonlinear interactions between runoff characteristics (depth, velocity, and duration) and hillslope attributes (length and gradient) [*Michaelides and Martin*, 2012], which determine the grain size fractions being transported, the rate of transport, and the distance. The simultaneous variation of rainfall intensity, duration, and infiltration rate affect the sediment transport characteristics of each hillslope differently, resulting in shifts to sediment supply fluctuations along the reach.

5.2. Supplied Sediment Sizes

Particle sizes of the modeled sediment supplied from the hillslopes fluctuate longitudinally and change significantly with intensity/duration of the rainfall. Figure 8 illustrates longitudinal patterns in the grain size enrichment ratio, ER (expressed as a ratio of the hillslope-supplied D_{50} to the initial hillslope D_{50}), which quantifies whether particles supplied to the channel are coarser (ER > 1) or finer (ER < 1) than those on the hillslope.

Three scenarios of potential grain size response to runoff can be identified: ER always < 1, ER always > 1, and ER fluctuating above and below 1. The two hillslopes that always produce an ER < 1 have contrasting attributes. One (at 14,235 m) is low gradient (10°) with average length (29 m), while the other (at 11,585 m) is the steepest (41°) and is very short (10 m). These two hillslopes consistently generate finer sediment than the initial hillslope D_{50} but for different reasons. The steep hillslope produces high runoff velocities with shallow flow depths, while the opposite occurs for the low-gradient hillslope. High runoff velocities under shallow

flows generate higher drag forces for partially submerged particles and higher drag and lift forces for fully submerged particles. On the low-gradient hillslope, the higher flow depths increase particle submersion in the flow, which raises lift forces relative to the shallow flows. Although the steep hillslope produces sediment loads an order of magnitude higher than the low-gradient hillslope, the hydraulic characteristics of the runoff in both cases are conducive to the transport of finer particles and hence both always have an ER < 1. The three hillslopes that always produce ER > 1 are extremely short (5, 6, and 10 m) and relatively steep (25°, 32°, and 30°). Despite their relatively low sediment loads across all rainfall events modeled, the combination of slopes with steep gradients and short lengths represents ideal runoff conditions for the transport of coarse fractions. The short length produces runoff accumulation over the whole slope even during low-duration rainfall (e.g., 3.75 min), and the steep gradient enables transport of the coarsest fraction. The remaining hillslopes are longer and of low to intermediate gradient, resulting in an ER that is more dependent on the specific rainfall duration, which controls runoff accumulation distance downslope and affects the transport distance of coarse particles within the slope [*Michaelides and Martin*, 2012]. Therefore, as rainfall duration and intensity change, the transport distance of the coarsest particles varies. When runoff accumulates over the whole slope, coarse particles are shed off the slope, resulting in a higher ER. However, when runoff accumulation distance is less than the slope length, the coarsest particles are deposited within the slope and ER is typically < 1. For these hillslopes, different hydrological conditions therefore manifest as fluctuating ER (above and below 1).

Therefore, the grain size supplied by hillslopes depends on the sensitivity of hillslopes to runoff. The most sensitive hillslopes, which display wide variations in grain size for different hydrological characteristics, tend to be long (most importantly) and low gradient (<20°). Length determines runoff accumulation downslope and therefore has a great impact on sediment transport distances. In dryland environments, where rainstorms tend to be short-lived (on the order of minutes) and runoff rarely reaches steady state on hillslopes, these effects can have a significant impact on sediment supply to the channel. This sensitivity decreases as hillslope gradient increases, and for very steep slopes, gradient effects dominate over hydrological variations. Short hillslopes, on the other hand, are more likely to reach hydrological equilibrium during shorter storms, so they are less sensitive to rainfall characteristics.

5.3. Modeled Hillslope-Supplied Particle Sizes Versus Measured Channel Particle Sizes

Figure 9a presents envelopes of modeled hillslope-supplied D_{10}, D_{50}, and D_{90} to the channel produced from all the hydrological scenarios, in relation to the measured in-channel particle sizes (D_{50} and D_{90}). Although longitudinal fluctuations in modeled grain sizes supplied from the hillslopes do not spatially correlate with fluctuations in measured channel grain sizes, the modeled supplied hillslope D_{50} and the measured channel D_{90} for the entire reach are statistically part of the same distribution (Kolmogorov-Smirnov statistic = 0.1992, $p = 0.72$, $n1/n2 = 18/29$). In other words, the signal of the median fraction (D_{50}) of sediment supplied by the hillslope is preserved in the coarse fraction of the channel grain sizes (D_{90}). There were no other statistical similarities between the three percentiles of modeled hillslope and measured in-channel sediment. One-to-one spatial correspondence is not expected because channels subsequently transport supplied sediment and sort grain sizes downstream. Nevertheless, between 8 and 10.5 km along the reach, there is a noticeable dip in the measured channel D_{50} and D_{90} in an area of the reach containing floodplains on both sides of the valley, which supports our modeling result on the role of floodplains in buffering coarse sediment supply from hillslopes.

Figure 9b compares global values of GSDs of modeled supplied hillslope sediment and measured channel sediment (lumped distributions for the entire reach). The modeled hillslope sediment supply is coarser overall than the measured channel sediment with a D_{50} of 36 mm compared to 25 mm. The supplied hillslope sediment GSD is finer at the tails than the original hillslope GSD. Although D_{50} remains the same (36 mm) the supplied sediment D_{10} and D_{90} are lower than the initial hillslope (D_{10}: 17 → 15 mm, D_{90}: 87 → 76 mm).

5.4. Impact of Hillslope Sediment Supply on the Channel

The results highlight hillslope responses to rainfall events of different intensities and durations, which vary significantly both in terms of sediment delivery to the channel and supplied sediment GSD. In many instances, the sediment load and GSD change in opposite directions—i.e., as sediment load increases, D_{50} decreases and vice versa. However, when considering the impact of hillslope sediment supply on the channel, one may assume that both load and grain size play a significant role. The total sediment load is

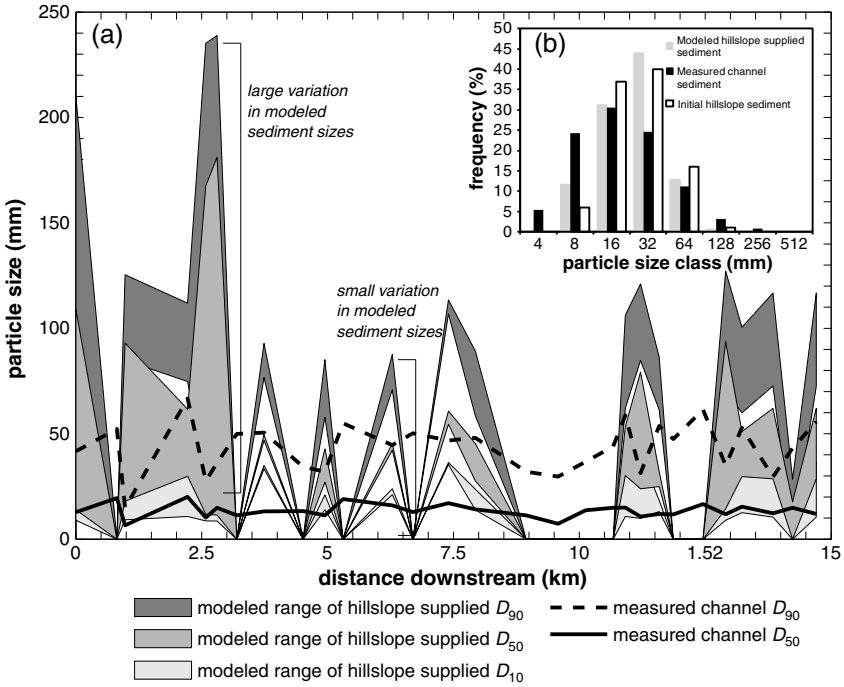

Figure 9. (a) Longitudinal variations in modeled hillslope-supplied grain sizes and measured channel grain sizes. Each of the shaded regions represents the range of modeled grain sizes (represented by the D_{10}, D_{50}, and D_{90}) supplied to the channel from the hillslope over all the rainfall/infiltration scenarios. Some hillslopes exhibit a large variation in supplied GSDs over the modeled hydrological scenarios while others consistently supply the same population of sediment sizes regardless of the hydrology. The black solid and dashed lines are the measured in-channel D_{10} and D_{50}, respectively. (b) Comparison of GSDs of measured channel sediment, modeled hillslope-supplied sediment to the channel, and initial hillslope sediment.

important because the mass of sediment supplied to the channel affects rates of valley fill and incision, while the GSD impacts bed load transport rates in the channel. In the absence of established theory on the impact of hillslope sediment supply on channels (but see M. B. Singer and K. Michaelides, How is topographic stability maintained in ephemeral, dryland channels? In Review, 2014), we heuristically assume that the total sediment mass supplied and grain size have equal weight and exert a first-order impact on the channel. We also assume that hillslope sediment supply impact is inversely proportional to channel width—the narrower the channel the higher the impact from the hillslopes, all other factors being equal. Hence, we propose the following index for the impact of hillslope supply on the channel (HSI, kg) that takes into account these three factors:

$$\mathrm{HSI} = \frac{\text{mass supplied} \cdot D_{50}}{W_{\mathrm{ch}}} \tag{5}$$

where mass supplied is the total sediment load supplied to the channel from a hillslope during a rainfall event (kg), D_{50} is the median grain size of the supplied sediment (m), and W_{ch} is the channel width (m). HSI is normalized to the maximum HSI across all modeled scenarios:

$$\mathrm{HSI}_* = \frac{\mathrm{HSI}}{\mathrm{HSI}_{\mathrm{max}}} \tag{6}$$

where $\mathrm{HSI}_{\mathrm{max}}$ is the maximum HSI (kg) over the range of modeled scenarios, HSI_* is the normalized HSI ($0 \le \mathrm{HSI}_* \le 1$). A $\mathrm{HSI}_* = 1$ denotes the largest impact of hillslope sediment supply on the channel within the basin for a range of rainstorms, while $\mathrm{HSI}_* = 0$ signifies no hillslope impact (zero sediment supply). We calculated HSI_* for all hillslope-channel cross sections and compared longitudinal patterns between all modeled rainfall/infiltration conditions (Figure 10). The results suggest that, for the same rainfall and infiltration rates, the impact of hillslope sediment supply on the channel decreases downstream. This occurs primarily as a result of the downstream increase in channel width because hillslope sediment flux

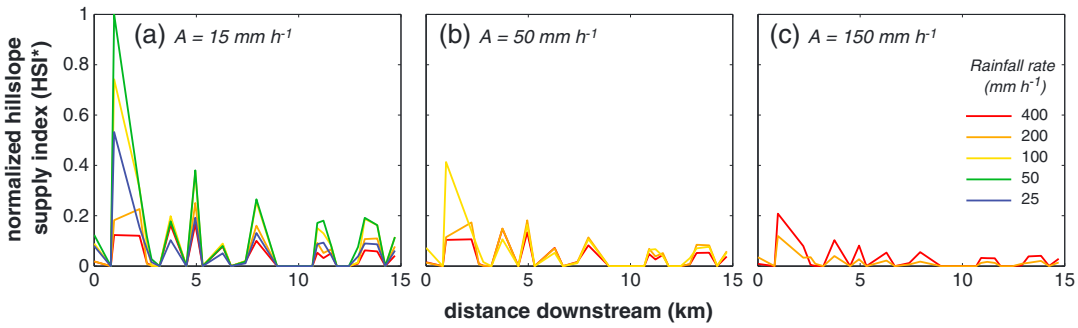

Figure 10. Longitudinal variations in normalized hillslope supply impact index (HSI*) for different rainfall intensities and durations for (a) $A = 15\ \mathrm{mm\ h^{-1}}$, (b) $50\ \mathrm{mm\ h^{-1}}$, and (c) $150\ \mathrm{mm\ h^{-1}}$, where A is final infiltration rate.

does not exhibit any decreasing longitudinal trends (Figure 7). Comparing Figures 7, 8, and 10 also shows that rainstorms which produce the highest hillslope impacts on the channel are the ones which deliver high sediment loads as well as relatively coarse sediment.

6. Discussion

A combined field- and modeling-based approach was used in this study to investigate the nature of coarse sediment supply from hillslopes to the channel in response to a range of rainfall events, and its potential impact on channel bed material within a dryland basin. Field measurements of sediment on the hillslopes and in the channel show that the hillslope surfaces are coarser than the channel bed material overall and suggest a combination of selective hillslope transport and/or in-channel sediment sorting. Longitudinal fluctuations in channel grain sizes within this ephemeral river (see Figure 9a) and the lack of any distinct downstream fining [*Rhoads*, 1989; *Thornes*, 1974, 1977] typically prevalent in perennial fluvial systems further suggest that hillslopes may play an important role in affecting longitudinal patterns of channel bed material in drylands and/or that processing of riverbed sediment during infrequent flash floods is incomplete and results in only partial sediment sorting (Singer and Michaelides, In Review). In this paper we investigate the potential contribution of hillslope sediment supply to the channel, and we do not account for in-channel processes. We also do not account for particle breakdown during hillslope transport, a likely important process in schist environments, which would contribute to the reduction in grain sizes. We place our emphasis on simulating runoff-driven hillslope sediment supply and associated GSDs to an ephemeral channel for a range of plausible rainfall events, which provides a clear vantage point to observe sediment inputs from lateral boundaries. Comparisons of modeled hillslope-supplied D_{50} with measured grain sizes in the channel revealed that channel D_{90} is the same order of magnitude as the modeled, hillslope-derived D_{50} (Figure 9a). This suggests that the coarse end of the channel GSD is composed of the average local hillslope input over a series of storm events, which is reasonable considering that the channel D_{90} would not be expected to move in most flood events. In other words, the hillslope supplies coarse bed material that remains in the channel bed as a lag deposit with longer residence times, leading to a good correspondence between the hillslope D_{50} and channel D_{90} over the reach. The channel D_{50} is more equivocal in terms of its origin. This population of channel grains is likely to be subjected to more substantial longitudinal sorting by floods than the coarse fraction, so while it may derive from the finer portions of hillslope input, we would not expect this to be based on simply local sediment supply from the slope.

Our modeling of coarse hillslope sediment supply along a 15 km reach illustrates discontinuous and fluctuating sediment inputs to the channel which are controlled by a combination of hillslope and rainfall attributes. The magnitude of spatial fluctuations (i.e., location of peak hillslope sediment supply and GSDs) and their longitudinal trends vary, depending on the hydrologic drivers such as rainfall intensity and duration, as well as steady state infiltration rates. Even under uniform infiltration, peaks in hillslope sediment supply within the reach are not always produced by the same rainfall event. Although the magnitude of the supply depends on interactions between hillslope gradient and rainfall characteristics, additional complexity is contributed by hillslope length, which results in nonlocal controls on sediment transport. Although hillslope gradient predominantly affects runoff flow velocity and particle gravitational forces, both of which

increase sediment flux, hillslope length determines the distance over which runoff accumulates and associated particle travel distances, especially during the nonequilibrium (short-duration) runoff events simulated here. Therefore, for hillslopes with similar gradients, different slope lengths can modulate the sediment supply to the channel, and the extent of this processing varies with rainfall intensity and duration.

Grain sizes supplied by the hillslope also fluctuate longitudinally but do not follow the same trend as sediment load. Some valley cross sections exhibit high variability in supplied grain size between the different rainfall events, while others show little change. The largest variation in both sediment load and grain sizes in relation to hydrologic changes is produced by long hillslopes, which are more dependent on the evolution of slope runoff hydraulics for transport of different grain sizes. Length affects runoff accumulation downslope (i.e., runoff increases partway downslope and levels off at a distance determined by storm duration), and coarse particles are deposited within the slope at that critical distance where runoff ceases to increase [see also *Michaelides and Martin*, 2012]. This sensitivity of long hillslopes to runoff becomes more pronounced as gradient decreases. In that sense, low-gradient, long hillslopes can therefore be considered most sensitive to rainfall variability. The lowest variation in supplied grain size is apparent on short and relatively steep hillslopes where gradient effects dominate sediment flux and where length does not play a strong role. In these cases, the short length enables runoff accumulation over most of the hillslope (i.e., runoff discharge increases linearly with distance) even during short-duration events and, in combination with the steep gradient, most grain size classes are transported all the way to the channel.

Despite the importance of hillslope sediment supply for channel GSD and bed load transport, there is a paucity of theoretical and modeling frameworks for addressing questions on the spatial and temporal distribution of sediment supply to the channel and its characteristics, especially with respect to climatic variations at the resolution of individual rainfall events. In this paper we present a heuristic measure of the impact of hillslope sediment supply on the channel (HSI_*), which takes into account hillslope sediment mass flux to the channel, D_{50} of supplied sediment, and the channel width for a valley section. Although simple and requiring field verification, HSI_* quantifies the relative impact of hillslope sediment supply to the channel for a range of hydrological scenarios. It can abstract the relative strength of hillslope impacts on the channel at a section, in a dynamic way, based on the magnitude and GSD of event-based sediment supply to the channel and their local impact as a function of channel width. Given that hillslopes, especially in drylands, respond in nonlinear ways to rainfall such that flux and grain sizes exhibit thresholds in relation to runoff and may change in different directions, it is challenging to determine how hillslope impacts vary within a basin and change in response to climate. The trends in HSI_* highlight some nonintuitive outcomes regarding which rainstorms are the most significant in terms of hillslope impacts on the channel. In this case, results show that total runoff is not a good predictor of hillslope impact on the channel (see, e.g., Figure 10a). Instead, they suggest that particular combinations of rainfall intensity and duration determine downslope runoff flow depths and velocities which, for different hillslopes, produce a characteristic balance between total sediment mass supplied and grain size distribution, which together have the highest local impact on the channel. This emergent behavior from the modeling occurs due to the interactions between hydrological and sediment transport drivers on the hillslopes involving the complex interplay of slope gradient effects (particle gravity forces, particle stability, flow velocity, and flow depth), slope length (runoff accumulation and particle transport distance), and grain size (relative particle submergence in flow and particle stability). In other words, a change in hillslope length and gradient affects both the hydrological characteristics which drive the sediment transport as well as the relative stability of sediment on the surface and the total transport distance to the channel.

6.1. Implications

There are several important implications of this research that warrant further discussion. First, our modeling framework for exploring the impacts of climatically controlled hillslope sediment supply in drylands may be suitable for incorporation into landscape evolution models (LEMs). Modeling the entire landscape remains an important goal in geomorphology (see *Tucker and Hancock* [2010] for a recent review), yet LEMs have some important shortcomings that limit their application on shorter (e.g., 10^1–10^4 years) timescales, over which colluvial/alluvial processes and behavior are often transient. LEM characterization of fluvial processes tends to be sophisticated compared with representation of hillslopes sediment generation, which is often based on geomorphic transport laws operating over long timescales [*Dietrich et al.*, 2003], rather than flow-driven processes occurring on an event basis. Even in cases where LEMs treat physical processes that link hillslopes to

channels [e.g., *Densmore et al*., 1998; *Gabet*, 2003], they are typically disconnected from the driving hydrology. There are examples where episodic mass wasting processes within a basin have been treated stochastically, which provides insight into transient patterns of sediment flux, storage, and channel morphology along the network based on climatic drivers [*Benda and Dunne*, 1997a, 1997b; *Gabet and Dunne*, 2003] or erosion rates, drainage density, concavity, and basin relief based on variability in rainfall [*Solyom and Tucker*, 2004; *Tucker and Slingerland*, 1997; *Tucker and Bras*, 2000]. However, these modeling frameworks typically assume perfect and universal coupling between hillslopes and channels, which we demonstrate here to be inappropriate for dryland fluvial systems. This paper addresses the problem of rainstorm-driven sediment supply in environments that are not dominated by mass wasting and where hillslopes and channels are not uniformly coupled throughout the drainage basin, which allows for direct investigation of transient behavior arising in alluvial channels.

Second, our findings and modeling show promise for improving understanding of longitudinal patterns of bed-material grain size, especially with respect to downstream fining [*Ferguson et al*., 1996; *Gasparini et al*., 2004; *Hoey and Ferguson*, 1994; *Ichim and Radoane*, 1990; *Paola and Seal*, 1995; *Singer*, 2008, 2010; *Yatsu*, 1955]. Evidence from a limited number of field studies of dryland channels suggests fluctuating grain sizes but no clear downstream fining [*Rhoads*, 1989; *Thornes*, 1974, 1977]. Other work has identified oscillations in dryland channel width [*Bull*, 1997; *Thornes*, 1974], which have been invoked to explain fluctuations in longitudinal patterns of aggradation and degradation [*Pelletier and DeLong*, 2004]. Our model results suggest that hillslope sediment supply provides the coarse component of riverbed material on a local basis. Thus, the local supply of sediment from hillslopes may dominate the character of dryland channels, as it apparently does in other mountainous environments [*Attal and Lave*, 2006]. The new framework for analyzing the dynamism associated with rainstorm-driven hillslope sediment supply in debris-mantled dryland basins may partly explain the absence of downstream fining and predominant grain size fluctuations in these systems. Furthermore, the model and the HSI_* index could aid in identifying which slopes are contributing to large fluctuations in longitudinal GSD by delivering large quantities of coarse bed material.

Third, this study may improve understanding of erosion rates in basins derived from cosmogenic radionuclides (CRNs). CRNs are widely applied to assess erosion rates over 10^2–10^7 year timescales [*Granger et al*., 2013]. Many of these studies analyze fluvial sediments to quantify basin-averaged erosion rates, but some attempt to gain insight into local erosion rates by sampling sediments on particular geomorphic surfaces, such as hillslopes [*Bierman and Nichols*, 2004; *Gosse and Phillips*, 2001]. Our research demonstrates that erosion is not uniform between hillslopes or even within individual hillslopes in dryland basins, which supports targeted sampling and analysis of CRNs from particular parts of a basin, in order to clarify the relationships between modern sediment yields and sediment production from the upland basin [e.g., *Bierman et al*., 2005; *Kirchner et al*., 2001]. More usefully, if our modeling were to be adapted to represent a range of potential rainfall events and their characterization in a stochastic treatment, the results would provide material for hypothesis generation on relative surface ages, which could be tested using CRNs to track these transient processes [*Willenbring et al*., 2013].

7. Conclusions

Sediment supply from hillslopes to channels is an important control on basin functioning and evolution. However, current theoretical frameworks do not adequately consider processes of runoff-driven hillslope sediment supply, which affects river channels at spatial and temporal scales that are different from discrete point sources of sediment that occur in soil-mantled landscapes (e.g., landslides). The importance of runoff-driven sediment supply is that it is sensitive to climatic variations and it is an intermittent yet significant source of sediment that impacts channels longitudinally. Complex interactions between hillslopes and climate at the level of individual rainstorms create challenges for understanding the extent of hillslope impacts on the channel in terms of sediment supply. In this paper, we use a combined field and modeling approach to quantify runoff-driven sediment supply to the channel in a dryland basin, where hillslopes are covered in coarse sediment and where infrequent rainstorms drive sediment transport processes. We applied a physics-based model to simulate longitudinal sediment supply to the channel based on measured valley cross sections for a series of plausible rainstorms of different intensities and durations. Finally, we developed a simple hillslope supply impact index which accounts for key sediment and channel characteristics.

Our results suggest that hillslope sediment supply to the channel is discontinuous and rainstorm dependent. Specifically, we found the following:

1. Modeled hillslope-supplied sediment mass and its GSD are determined by the nonlinear interaction between rainfall characteristics and hillslope attributes, resulting in longitudinal fluctuations in supply, the relative magnitude, and location of which varies between storms.
2. Floodplains buffer coarse sediment supply from hillslopes.
3. The measured channel grain sizes fluctuate longitudinally and do not exhibit downstream fining.
4. Our modeled hillslope-supplied D_{50} is mirrored in the measured in-channel D_{90}.
5. Our hillslope supply impact index provides new insights into which rainstorms have potentially the most impact on the supply of hillslope sediment to the channel.

Our results suggest that hillslopes exert a significant control on channel bed material in coarse-mantled dryland basins and have important implications for understanding climatic controls on basin functioning, landscape evolution, and the relationship between hillslope attributes and differential erosion rates.

Acknowledgments
Gareth J. Martin collected the hillslope particle size data. The aerial photographs in Figure 2a were kindly provided by Nick Drake (King's College London). We thank Dan Hobley and two anonymous reviewers for helpful comments on the original manuscript. Please contact the corresponding author for data inquiries.

References

Armitage, J. J., R. A. Duller, A. C. Whittaker, and P. A. Allen (2011), Transformation of tectonic and climatic signals from source to sedimentary archive, *Nat. Geosci.*, *4*(4), 231–235.

Attal, M., and J. Lave (2006), Changes of bedload characteristics along the Marsyandi River (central Nepal): Implications for understanding hillslope sediment supply, sediment load evolution along fluvial networks, and denudation in active orogenic belts, in *Tectonics, Climate, and Landscape Evolution*, edited by S. D. Willett et al., pp. 143–171, Geological Soc Amer Inc, Boulder.

Benda, L., and T. Dunne (1997a), Stochastic forcing of sediment routing and storage in channel networks, *Water Resour. Res.*, *33*(12), 2865–2880, doi:10.1029/97WR02387.

Benda, L., and T. Dunne (1997b), Stochastic forcing of sediment supply to channel networks from landsliding and debris flow, *Water Resour. Res.*, *33*(12), 2849–2863, doi:10.1029/97WR02388.

Bierman, P. R., and K. K. Nichols (2004), Rock to sediment-slope to sea with 10-Be-rates of landscape change, *Annu. Rev. Earth Planet. Sci.*, *32*, 215–255.

Bierman, P. R., J. M. Reuter, M. Pavich, A. C. Gellis, M. W. Caffee, and J. Larsen (2005), Using cosmogenic nuclides to contrast rates of erosion and sediment yield in a semi-arid, arroyo-dominated landscape, Rio Puerco Basin, New Mexico, *Earth Surf. Process. Landf.*, *30*(8), 935–953, doi:10.1002/esp.1255.

Blott, S. J., and K. Pye (2001), GRADISTAT: A grain size distribution and statistics package for the analysis of unconsolidated grains, *Earth Surf. Process. Landf.*, *26*, 1237–1248.

Bracken, L. J., N. J. Cox, and J. Shannon (2008), The relationship between rainfall inputs and flood generation in south-east Spain, *Hydrol. Process.*, *22*(5), 683–696, doi:10.1002/hyp.6641.

Bull, L. J., M. J. Kirkby, J. Shannon, and J. M. Hooke (1999), The impact of rainstorms on floods in ephemeral channels in southeast Spain, *Catena*, *38*, 191–209.

Bull, W. B. (1997), Discontinuous ephemeral streams, *Geomorphology*, *19*(3–4), 227–276.

Carson, M. A., and M. J. Kirkby (1972), *Hillslope Form and Processes*, 475 pp. Cambridge Univ. Press, Cambridge.

Carson, M. A., C. H. Taylor, and B. J. Grey (1973), Sediment production in a small Appalachian watershed during spring runoff: The Eaton Basin, 1970–1972, *Can. J. Earth Sci.*, *10*(12), 1707–1734.

Densmore, A. L., M. A. Ellis, and R. S. Anderson (1998), Landsliding and the evolution of normal-fault-bounded mountains, *J. Geophys. Res.*, *103*(B7), 15,203–15,219, doi:10.1029/98JB00510.

Dietrich, W. E., J. W. Kirchner, H. Ikeda, and F. Iseya (1989), Sediment supply and the development of the coarse surface layer in gravel-bedded rivers, *Nature-letter*, *340*, 215–217.

Dietrich, W. E., D. G. Bellugi, L. S. Sklar, J. D. Stock, and A. M. Heimsath (2003), Geomorphic transport laws for predicting landscape form and dynamics, in *Prediction in Geomorphology*, edited by P. R. Wilcock and R. M. Iverson, AGU, Washington, D. C.

Ferguson, R., T. Hoey, S. Wathen, and A. Werrity (1996), Field evidence for rapid downstream fining of river gravels through selective transport, *Geology*, *24*(2), 179–182.

Gabet, E. J. (2003), Sediment transport by dry ravel, *J. Geophys. Res.*, *108*(B1), 2049, doi:10.1029/2001jb001686.

Gabet, E. J., and T. Dunne (2003), A stochastic sediment delivery model for a steep Mediterranean landscape, *Water Resour. Res.*, *39*(9), 1237, doi:10.1029/2003WR002341.

Gasparini, N. M., G. E. Tucker, and R. L. Bras (2004), Network-scale dynamics of grain-size sorting: Implications for downstream fining, stream-profile concavity, and drainage basin morphology, *Earth Surf. Process. Landf.*, *29*(4), 401–421.

Gilbert, G. K. (1914), The transportation of debris by running water, Professional Paper, US Geol. Sur., Menlo Park, Calif.

Gilbert, G. K. (1917), Hydraulic-mining debris in the Sierra Nevada, Professional Paper, US Geological Survey Professional Paper 105, Menlo Park, Calif.

Gomez, B., B. J. Rosser, D. H. Peacock, D. M. Hicks, and J. A. Palmer (2001), Downstream fining in a rapidly aggrading gravel bed river, *Water Resour. Res.*, *37*(6), 1813–1823, doi:10.1029/2001WR900007.

Gosse, J. C., and F. M. Phillips (2001), Terrestrial in situ cosmogenic nuclides: Theory and application, *Quat. Sci. Rev.*, *20*(14), 1475–1560.

Granger, D. E., N. A. Lifton, and J. K. Willenbring (2013), A cosmic trip: 25 years of cosmogenic nuclides in geology, *Geol. Soc. Am. Bull.*, doi:10.1130/b30774.1.

Green, W. H., and G. A. Ampt (1911), Studies on soil physics. Part I. The flow of air and water through soils, *J. Agric. Sci.*, *4*(1), 1–24.

Harvey, A. M. (1991), The influence of sediment supply on the channel morphology of upland streams: Howgill Fells, Northwest England, *Earth Surf. Process. Landf.*, *16*(7), 675–684.

Harvey, A. M. (2001), Coupling between hillslopes and channels in upland fluvial systems: Implications for landscape sensitivity, illustrated from the Howgill Fells, northwest England, *Catena*, *42*(2–4), 225–250.

Harvey, A. M. (2002), Effective timescales of coupling within fluvial systems, *Geomorphology*, *44*(3–4), 175–201.
Hicks, D. M., B. Gomez, and N. A. Trustrum (2000), Erosion thresholds and suspended sediment yields, Waipaoa River Basin, New Zealand, *Water Resour. Res.*, *36*(4), 1129–1142, doi:10.1029/1999wr900340.
Hoey, T. B., and R. I. Ferguson (1994), Numerical simulation of downstream fining by selective transport in gravel bed rivers: Model development and illustration, *Water Resour. Res.*, *30*(7), 2251–2260, doi:10.1029/94WR00556.
Hoey, T. B., and R. I. Ferguson (1997), Controls of strength and rate of downstream fining above a river base level, *Water Resour. Res.*, *33*(11), 2601–2608, doi:10.1029/97WR02324.
Hovius, N., C. P. Stark, and P. A. Allen (1997), Sediment flux from a mountain belt derived by landslide mapping, *Geology*, *25*(3), 231–234.
Hovius, N., C. P. Stark, H. T. Chu, and J. C. Lin (2000), Supply and removal of sediment in a landslide-dominated mountain belt: Central Range, Taiwan, *J. Geol.*, *108*(1), 73–89.
Ichim, I., and M. Radoane (1990), Channel sediment variability along a river: A case study of the Siret River (Romania), *Earth Surf. Process. Landf.*, *15*(3), 211–225.
Iseya, F., and H. Ikeda (1987), Pulsations in bedload transport rates induced by a longitudinal sediment sorting: A flume study using sand and gravel mixtures, *Geogr. Ann.*, *69*(1A), 15–27.
Kirchner, J. W., W. E. Dietrich, F. Iseya, and H. Ikeda (1990), The variability of critical shear stress, friction angle, and grain protrusion in water-worked sediments, *Sedimentology*, *37*, 647–672.
Kirchner, J. W., R. C. Finkel, C. S. Riebe, D. E. Granger, J. L. Clayton, J. G. King, and W. F. Megahan (2001), Mountain erosion over 10 yr, 10 k.y., and 10 m.y. time scales, *Geology*, *29*(7), 591–594.
Knighton, A. D. (1989), River adjustment to changes in sediment load: The effects of tin mining on the Ringarooma River, Tasmania, 1875-1984, *Earth Surf. Process. Landf.*, *14*, 333–359.
Komar, P. D., and Z. Li (1986), Pivoting analyses of the selective entrainment of sediments by shape and size with application to gravel threshold, *Sedimentology*, *33*(3), 425–436.
Korup, O., A. L. Densmore, and F. Schlunegger (2010), The role of landslides in mountain range evolution, *Geomorphology*, *120*(1–2), 77–90, doi:10.1016/j.geomorph.2009.09.017.
Li, Z., and P. D. Komar (1986), Laboratory measurements of pivoting angles for applications to selective entrainment of gravel in a current, *Sedimentology*, *33*, 413–423.
Lisle, T., J. Pizzuto, H. Ikeda, F. Iseya, and Y. Kodoma (1997), Evolution of a sediment wave in an experimental channel, *Water Resources Res*, *33*(8), 1971–1981.
Lisle, T. E., F. Iseya, and H. Ikeda (1993), Response of a channel with alternate bars to a decrease in supply of mixed-size bed load: A flume experiment, *Water Resour. Res.*, *29*(11), 3623–3629, doi:10.1029/93WR01673.
Lisle, T. E., Y. Cui, G. Parker, J. E. Pizzuto, and A. M. Dodd (2001), The dominance of dispersion in the evolution of bed material waves in gravel-bed rivers, *Earth Surf. Process. Landf.*, *26*, 1409–1420.
Madej, M. A., and V. Ozaki (1996), Channel response to sediment wave propagation and movement, Redwood Creek, California, USA, *Earth Surf. Process. Landf.*, *21*(10), 911–927.
Michaelides, K., and J. Wainwright (2002), Modelling the effects of hillslope-channel coupling on catchment hydrological response, *Earth Surf. Process. Landf.*, *27*(13), 1441–1457, doi:10.1002/esp.440.
Michaelides, K., and M. D. Wilson (2007), Uncertainty in predicted runoff due to patterns of spatially variable infiltration, *Water Resour. Res.*, *43*, W02415, doi:10.1029/2006wr005039.
Michaelides, K., and J. Wainwright (2008), Internal testing of a numerical model of hillslope-channel coupling using laboratory flume experiments, *Hydrol. Process.*, *22*(13), 2274–2291, doi:10.1002/hyp.6823.
Michaelides, K., and G. J. Martin (2012), Sediment transport by runoff on debris-mantled dryland hillslopes, *J. Geophys. Res.*, *117*, F03014, doi:10.1029/2012JF002415.
Miller, R. L., and R. J. Byrne (1966), The angle of repose for a single grain on a fixed rough bed, *Sedimentology*, *6*, 303–314.
Nichols, M. H., M. A. Nearing, V. O. Polyakov, and J. J. Stone (2013), A sediment budget for a small semiarid watershed in southeastern Arizona, USA, *Geomorphology*, *180–181*, 137–145, doi:10.1016/j.geomorph.2012.10.002.
Nicholson, S. E. (2011), *Dryland Climatology*, 1st ed., Cambridge Univ. Press, Cambridge.
Paola, C., P. L. Heller, and C. L. Angevine (1992), The large-scale dynamics of grain-size variation in alluvial basins, 1: Theory, *Basin Res.*, *4*, 73–90.
Paola, C., and R. Seal (1995), Grain size patchiness as a cause of selective deposition and downstream fining, *Water Resour. Res.*, *31*, 1395–1407, doi:10.1029/94WR02975.
Pelletier, J. D., and S. DeLong (2004), Oscillations in arid alluvial-channel geometry, *Geology*, *32*(8), 713–716, doi:10.1130/g20512.1.
Rhoads, B. L. (1989), Longitudinal variations in the size and sorting of bed material along 6 arid-region mountain streams, *Catena*, *14*, 87–105.
Rice, S. (1998), Which tributaries disrupt downstream fining along gravel-bed rivers?, *Geomorphology*, *22*, 39–56.
Rice, S. (1999), The nature and controls on downstream fining within sedimentary links, *J. Sediment. Res.*, *69*(1), 32–39.
Rustomji, P., and I. Prosser (2001), Spatial patterns of sediment delivery to valley floors: Sensitivity to sediment transport capacity and hillslope hydrology relations, *Hydrol. Process.*, *15*(6), 1003–1018, doi:10.1002/hyp.231.
Scoging, H. M. (1992), Modelling overland flow hydrology for dynamic hydraulics, in *Overland Flow: Hydraulics and Erosion Mechanics*, edited by A. J. Parsons and A. D. Abrahams, pp. 89–103, UCL Press, London.
Singer, M. B. (2008), Downstream patterns of bed-material grain size in a large, lowland alluvial river subject to low sediment supply, *Water Resour. Res.*, *44*, W12202, doi:10.1029/2008WR007183.
Singer, M. B. (2010), Transient response in longitudinal grain size to reduced gravel supply in a large river, *Geophys. Res. Lett.*, *37*, L18403, doi:10.1029/2010gl044381.
Solyom, P. B., and G. E. Tucker (2004), Effect of limited storm duration on landscape evolution, drainage basin geometry, and hydrograph shapes, *J. Geophys. Res.*, *109*, F03012, doi:10.1029/2003jf000032.
Thornes, J. B. (1974), *Speculation on the Behaviour of Stream Channel Width*, London School of Economics, London.
Thornes, J. B. (1977), Channel change in ephemeral streams: Observations, problems and models, in *River Channel Changes*, edited by K. G. Gregory, pp. 317–335, John Wiley, Chichester.
Thornes, J. B., and A. Gilman (1983), Potential and actual erosion around archaeological sites in south-east Spain, in *Rainfall Simulation, Runoff and Soil Erosion*, edited by J. d. Ploey, pp. 91–113, Catena, Reiskirchen, Germany.
Tucker, G. E., and R. Slingerland (1997), Drainage basin responses to climate change, *Water Resour. Res.*, *33*(8), 2031–2047, doi:10.1029/97WR00409.
Tucker, G. E., and R. L. Bras (2000), A stochastic approach to modeling the role of rainfall variability in drainage basin evolution, *Water Resour. Res.*, *36*(7), 1953–1964, doi:10.1029/2000WR900065.

Tucker, G. E., and G. R. Hancock (2010), Modelling landscape evolution, *Earth Surf. Process. Landf.*, *35*(1), 28–50, doi:10.1002/esp.1952.
Venditti, J. G., W. E. Dietrich, P. A. Nelson, M. A. Wydzga, J. Fadde, and L. Sklar (2010), Mobilization of coarse surface layers in gravel-bedded rivers by finer gravel bed load, *Water Resour. Res.*, *46*, W07506, doi:10.1029/2009wr008329.
Willenbring, J. K., N. M. Gasparini, B. T. Crosby, and G. Brocard (2013), What does a mean mean? The temporal evolution of detrital cosmogenic denudation rates in a transient landscape, *Geology*, doi:10.1130/g34746.1.
Wolman, M. G. (1954), A method of sampling coarse river-bed material, *Trans., Am. Geophys. Union*, *35*(6), 951–956.
Yair, A., D. Sharon, and H. Lavee (1978), An instrumented water-shed for the study of partial area contribution of runoff in the arid zone, *Z. Geomorphol. Supp.*, *29*, 71–82.
Yatsu, E. (1955), On the longitudinal profile of the graded river, *Trans., Am. Geophys. Union*, *36*(4), 211–219.